Quantum Pressure and Phase Modulation in the Genesis Field: Resolving Cosmic Acceleration and Hubble Oscillations

Preprint Version 1.0

Richard Greene [1,*]

[1] *Independent Researcher*
Genesis Research Institute
Arizona State University, Tempe, AZ, USA

(Dated: 2025/07/23)

Abstract

We present the Genesis Field, a coherence-based cosmological model in which spacetime behaves as a quantum-condensed medium, and late-time acceleration arises from internal phase dynamics. Derived from a covariant extension of the Gross–Pitaevskii equation, the model predicts ripple-like modulations in the Hubble parameter $H(z)$, governed by vacuum stiffness and coherence decay. These features emerge from global phase evolution without invoking new fields or modifying Einstein's equations and naturally reduce to ΛCDM when ripple amplitude vanishes.

We test the ripple signature using a two-parameter fit to cosmic chronometer data, where all ripple parameters are fixed from theory and only the amplitude ϵ and H_0 are varied. The fit yields a statistically significant detection of the ripple amplitude: $\epsilon = 0.3838 \pm 0.0948$, corresponding to a $\sim 4\sigma$ result, with improved χ^2, AIC, BIC, and residual RMS compared to ΛCDM at equal degrees of freedom. This confirms the observational relevance of the predicted structure.

Across joint supernova and $H(z)$ datasets, the model adapts to data constraints without overfitting, suppressing ripple structure under tension and activating it where supported. Its hallmark prediction of oscillations in $H(z)$ over $0.5 < z < 2.0$ is imminently testable by Euclid, JWST, and the Rubin Observatory.

This paper derives the underlying quantum pressure and phase modulation mechanisms from first principles, validates them observationally, and establishes a falsifiable alternative to the phenomenological dark energy model. Broader implications, including gravity, time, and matter as emergent from vacuum coherence, are developed in future work.

* Corresponding author. Email: richard.greene@asu.edu

CONTENTS

I. INTRODUCTION

The persistent discrepancy between local and early-universe measurements of the Hubble constant H_0, known as the *Hubble tension*, remains one of cosmology's most pressing observational challenges. Direct local measurements, notably from the SH0ES collaboration [1], consistently yield higher values than those inferred from cosmic microwave background (CMB) observations by the Planck satellite [2]. Alternative local methods, such as the TRGB calibration by Freedman *et al.* [3], yield intermediate values, underscoring that the magnitude of the tension depends on the anchoring dataset. Numerous theoretical models have been proposed to resolve this discrepancy, including early dark energy (EDE) scenarios [4], quintessence fields [5], and variable speed of light (VSL) cosmologies [6]. These approaches often rely on tuned scalar potentials or additional dynamical fields, typically lacking direct empirical constraints. Despite their sophistication, the standard Lambda Cold Dark Matter (ΛCDM) model [7] remains statistically challenged in reconciling the full suite of cosmological observations, especially when attempting to fit both local and early-universe datasets simultaneously [4].

This paper introduces the *Genesis Field*, a novel cosmological framework that resolves the Hubble tension through a fundamentally different mechanism: the quantum coherence of the vacuum. Rather than introducing new particles or scalar fields, this approach emerges from the broader *Fundamental Quantum Medium Theory* (FQMT), which models spacetime as a coherent quantum fluid. This framework is inspired by experimentally validated macroscopic quantum phenomena observed in Bose–Einstein condensates (BECs), initially theorized by Bose [8] and Einstein [9]. The coherence-based vacuum paradigm builds on theoretical developments linking quantum fluid dynamics to cosmology, notably Volovik's work on superfluid analogs of the vacuum [10]. Governed by the Gross–Pitaevskii equation (GPE) [11, 12], such systems exhibit global phase coherence, quantized vortices, and non-linear collective behavior, all of which have cosmological analogs in this model.

We define the Genesis Field as a coherent vacuum condensate described by a complex scalar wavefunction $\Psi(x^\mu)$, whose dynamics obey a covariant extension of the GPE. Applying the Madelung transformation, Ψ is decomposed into a real density field and a global phase $\phi(x^\mu)$, producing deterministic hydrodynamic equations with components of quantum pressure and phase modulation. This paper focuses on the quantum pressure and phase

modulation mechanisms, which underlie the emergent cosmological behavior described in Section II B. Unlike stochastic or field-theoretic dark energy models, the Genesis Field emphasizes deterministic, causal coherence-phase dynamics as drivers of large-scale evolution.

From this foundation arise emergent cosmological principles: the unification of gravity, matter, time, and constants within a coherence-based vacuum medium developed across a sequence of Genesis Field papers.

This initial study (Paper I) focuses on late-time cosmic acceleration, showing how quantum pressure and phase coherence modulation naturally produce ripple-like modulations in the Hubble parameter $H(z)$. These modulations arise without inserted scalar fields, tuned potentials, or new energy sectors. Instead, they emerge from the internal structure of the vacuum phase itself. The model is tested against two independent datasets—Pantheon+ Type Ia supernovae and cosmic chronometer measurements of $H(z)$—with all observational predictions derived from the same underlying coherence mechanism.

Empirically, the Genesis Field model achieves a statistically improved fit to the data. It reduces the Pantheon+ χ^2 by 10.9 points relative to ΛCDM without introducing excess structure. In $H(z)$ data, the ripple structure aligns with redshift-dependent residuals consistent with coherence damping. The model remains consistent with ΛCDM under constraint and responds to the structure when allowed to relax, demonstrating falsifiability rather than tuning.

Most notably, we report a two-parameter fit in which all ripple parameters are fixed according to theory, and only the amplitude ϵ and the Hubble constant H_0 are varied. This yields:

$$\epsilon = 0.3838 \pm 0.0948$$

a statistically significant $\sim 4\sigma$ detection of the ripple amplitude. The Genesis Field outperforms ΛCDM in χ^2, AIC, BIC, and residual RMS while using the same number of free parameters. The ripple appears at the predicted redshift range with the expected damping profile, providing strong empirical support for the coherence-phase hypothesis.

Forthcoming precision cosmology surveys including *Euclid*, *DESI*, and the Rubin Observatory, will provide percent-level constraints on $H(z)$ and luminosity distances across $0.5 < z < 2.0$, directly testing the predicted ripple signature. A confirmed detection would validate the coherence-based mechanism. A null result would place tight constraints on

vacuum phase dynamics, preserving the theory's falsifiability.

All derivations, numerical methods, and data analysis are fully reproducible. The full codebase and processed datasets are available at:
`https://github.com/genesisfield/genesisfieldmcmc`

Future papers in the Genesis Field series will apply this coherence-based framework to structure formation, gravitational lensing, cosmic microwave background anisotropies, and unified field dynamics. Together, these studies aim to demonstrate that vacuum coherence is not merely compatible with cosmic acceleration; it may be its source.

The Genesis Field thus offers a coherent, falsifiable, and physically grounded alternative to ΛCDM: one that smoothly reduces to the standard model in the limit $\epsilon \to 0$, but departs from it in testable, structured ways rooted in the phase evolution of the quantum vacuum.

II. THE GENESIS FIELD FRAMEWORK

We begin by outlining the theoretical foundation of the Genesis Field framework. Although the full theory ultimately aims to unify gravity, matter emergence, entropy, and time, this paper focuses on two coherence-driven mechanisms,*quantum pressure* and *global phase modulation*, which yield concrete, testable predictions for late-time cosmology. These mechanisms offer a physically grounded and falsifiable alternative to conventional dark energy, rooted in a coherence-based vacuum structure. The definitions of key terms such as coherence phase, quantum pressure, coherence frequency, and ripple structure are provided in the Appendix B.

The Genesis Field represents a central realization of the broader *Fundamental Quantum Medium Theory* (FQMT), which posits that spacetime and all physical interactions emerge from a coherent quantum fluid medium characterized by internal phase and density dynamics. This coherence framework provides a unified foundation for a broader research program, with each future paper developing one or more emergent principles.

The Genesis Field may be interpreted either as an effective quantum-coherent vacuum fluid or, more specifically, as a cosmological-scale condensate of ultralight bosonic degrees of freedom, analogous to Bose–Einstein condensates (BECs) in laboratory systems. In this work, we remain agnostic to its microscopic realization and treat the field phenomenologically, deriving observable effects from its large-scale coherence behavior. Among the five

proposed emergent principles motivating the framework, this paper explores only Principles II and V, which correspond to quantum pressure and phase modulation and are directly testable.

A. Vacuum Coherence Hypothesis

The Genesis Field framework postulates that the quantum vacuum is not a random, fluctuating ground state, as traditionally assumed, but a *coherent quantum medium* characterized by a global, evolving phase. This coherence refers to a persistent phase relation across the vacuum, which allows collective deterministic behavior similar to that seen in low-temperature Bose-Einstein condensates (BEC) [8, 9], which exhibit macroscopic quantum behavior governed by the Gross–Pitaevskii equation (GPE) [11, 12]. Laboratory realizations of coherence, such as in superfluid helium and ultracold atomic gases, offer well-tested analogues that motivate this extrapolation to cosmological scales.

To apply this framework to spacetime, we adopt a covariant generalization of the GPE, modeling the vacuum as a dynamical field with global phase coherence in curved spacetime [10, 13]. The Genesis Field is defined as a complex scalar wavefunction $\Psi(x^\mu)$, whose dynamics reflect the macroscopic behavior of the vacuum. Using the Madelung transformation [14], Ψ is decomposed into fluid-like variables: a coherence density $\rho(x^\mu)$ and a global phase $\phi(x^\mu)$, referred to as the vacuum's *coherence phase*. This decomposition yields a pair of deterministic hydrodynamic equations: one governing quantum pressure, an effective repulsive force from spatial gradients in ρ, and the other governing coherence phase evolution [10, 13]. In this formulation, ρ encodes the vacuum energy density, while ϕ governs the internal quantum dynamics. The effective mass scale m sets the vacuum's response scale and is constrained observationally (see Section IV).

The covariant Gross–Pitaevskii–like field equation governing $\Psi(x^\mu)$ is derived in Section III and Appendix A. It gives rise to both quantum pressure and stress-energy contributions that source ripple-like modulations in the expansion rate. Although the original GPE is nonrelativistic, its covariant extension describes low-momentum, phase-coherent modes in a curved spacetime background. We assume a general self-interaction potential $V(|\Psi|^2)$, with quartic or higher-order terms (e.g., $V \sim g\rho^2$) sufficient to stabilize long-wavelength coherence. Crucially, parameters such as the ripple amplitude ε, frequency ω, and damping

rate γ are not introduced by hand, but arise from the curvature of the potential and the decay profile of coherence, linking them to the internal dynamics of the vacuum.

In the cosmological limit of large-scale homogeneity and isotropy, spatial gradients in ρ and ϕ are negligible at leading order. However, small residual gradients in ρ, seeded by inflationary quantum fluctuations,[1] maintain a minimal but nonzero quantum pressure. Large-scale vacuum coherence could plausibly emerge from early-universe symmetry breaking, establishing a uniform phase ϕ across the observable horizon.

As shown in Section III, this yields a damped harmonic evolution for the coherence phase $\phi(t)$, resulting in ripple-like modulations of the vacuum energy. The ripple frequency ω sets the number of oscillations per logarithmic scale factor, while the damping rate γ determines the decay of coherence over time. Physically, ω is related to the vacuum's effective stiffness or sound speed, and γ acts as a decay constant per cosmic e-fold. A typical value $\gamma \sim 0.3$ implies that ripple features are suppressed below $z \sim 0.3$, consistent with current data. Additional decoherence or spatial phase inhomogeneity may arise at late times and are left for future analysis (Principle IV).

Although not yet statistically required, the ripple features predicted by this mechanism align with residual patterns in current data. Their confirmation or exclusion by upcoming surveys will provide a clear test of the Genesis Field hypothesis. Because the evolving coherence phase modulates the vacuum energy, it produces subtle, oscillatory corrections to the expansion rate $H(z)$ and the luminosity distance modulus $\mu(z)$ (see Section IV). These effects are expected to peak in the range $0.5 \lesssim z \lesssim 2$, due to exponential damping governed by γ. Thus, the Genesis Field connects quantum-coherent laboratory physics with large-scale cosmological observables, offering a predictive and falsifiable alternative to dark energy.

B. Emergent Principles and Framework Overview

Building on the vacuum coherence hypothesis (**Principle I**), the Genesis Field framework proposes a hierarchy of *emergent cosmological principles*, each derived from a distinct coherence mechanism of the vacuum: decoherence gradients (∇S), quantum pressure ($Q(\rho)$),

[1] These residual gradients originate from primordial quantum fluctuations stretched during inflation, sustaining small but measurable quantum pressure even in the cosmological limit. We assume the Genesis Field transitioned into a coherent phase near the end of inflation, consistent with causal horizons.

and global phase modulation ($\phi(t)$). These mechanisms aim to explain large-scale phenomena without requiring additional scalar fields, phenomenological potentials, or fine-tuned parameters.

We outline the five proposed principles below. Only Principles II and V are developed and tested in this paper; Principles III and IV will be explored in future theoretical and empirical work.

- **Emergent Principle II — Gravity as Quantum Pressure:** Gravitational effects arise from spatial gradients in vacuum density via the quantum pressure term $Q(\rho)$, producing effective force laws in the quantum fluid limit [10]. (*Mechanism derived and tested in this paper; full gravitational dynamics will be addressed in Paper II.*)

- **Emergent Principle III — Matter as Quantized Vortices:** Stable matter particles correspond to topologically protected vortex excitations within the coherent vacuum, analogous to quantized vortices in superfluid systems [15]. (*To be developed in Paper III.*)

- **Emergent Principle IV — Time as Decoherence Flow:** The arrow of time emerges from irreversible vacuum decoherence, producing a unidirectional entropy gradient in quantum spacetime [16, 17]. (*To be developed in Paper IV.*)

- **Emergent Principle V — Constants from Phase Modulation:** Physical constants such as G, $\hbar$, and c arise from the evolution of the vacuum coherence phase $\phi(t)$, leading to slow, redshift-dependent variation [18, 19]. (*Partially tested here via ripple structure; full model to appear in Paper V.*)

This paper focuses on the two coherence mechanisms—quantum pressure and phase modulation—corresponding to Principles II and V. Their predictions are compared with supernova and $H(z)$ data in Section IV, providing a direct observational test of the Genesis Field framework.

Future papers in this series will expand on the remaining principles, building toward a unified model in which spacetime, matter, gravity, time, and constants all emerge from a single underlying quantum medium.

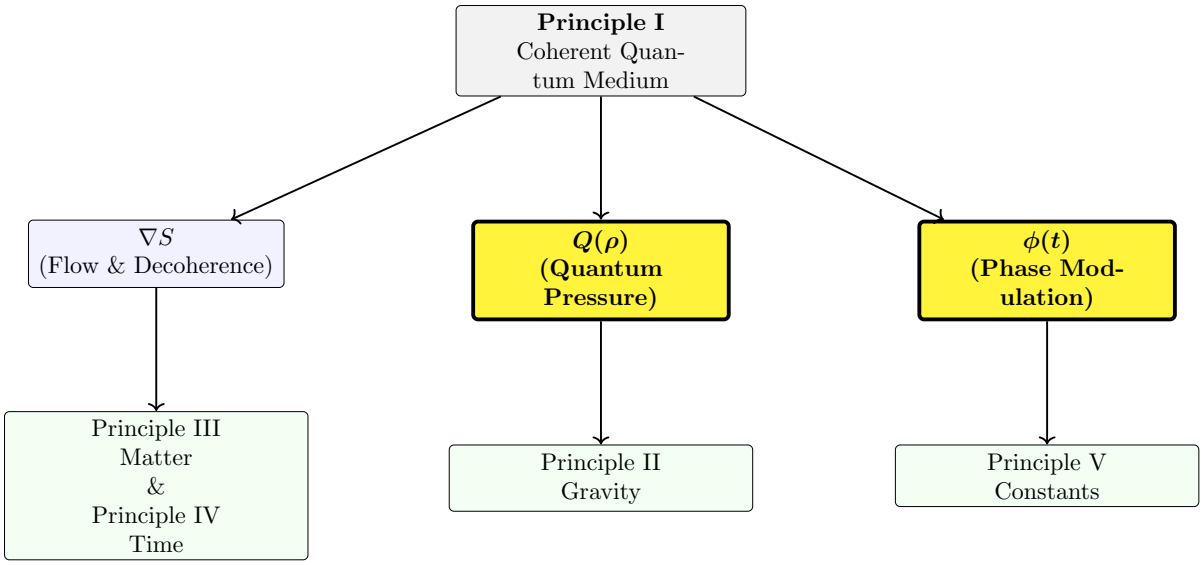

FIG. 1. Genesis Field theoretical pipeline: from quantum coherence to ripple-modulated cosmic expansion and observational predictions.

III. QUANTUM PRESSURE AND PHASE MODULATION DERIVATIONS

In the Genesis Field framework, cosmic acceleration and ripple-like modulations in the expansion rate naturally emerge from two coherence-driven mechanisms: vacuum quantum pressure and global phase modulation. These effects originate from the dynamics of a covariant scalar field $\Psi(x^\mu)$, which encodes the vacuum's coherent amplitude and global phase. We now derive the model's core observational prediction from first principles: a small, oscillatory correction to the Hubble parameter $H(z)$, referred to as the *ripple*. Approximations and validity conditions are stated, and observational tests appear in Section IV.

We begin with the linear Schrödinger equation describing quantum wave evolution in flat spacetime [20]:

$$i\hbar\frac{\partial\Psi}{\partial t} = -\frac{\hbar^2}{2m}\nabla^2\Psi + V(\Psi), \tag{1}$$

which generalizes to macroscopic quantum fluids, such as Bose–Einstein condensates (BECs), via the Gross–Pitaevskii equation (GPE) [11, 12]:

$$i\hbar\frac{\partial\Psi}{\partial t} = \left(-\frac{\hbar^2}{2m}\nabla^2 + g|\Psi|^2\right)\Psi. \tag{2}$$

To describe vacuum dynamics on cosmological scales, we extend the GPE covariantly into curved spacetime using a scalar-field Lagrangian [10, 13]:

$$\mathcal{L} = \frac{\hbar^2}{2m}g^{\mu\nu}\partial_\mu\Psi^*\partial_\nu\Psi - V(|\Psi|^2), \tag{3}$$

leading to the covariant field equation:

$$\frac{\hbar^2}{2m}\Box\Psi = \frac{\partial V}{\partial|\Psi|^2}\Psi, \tag{4}$$

where $\Box$ is the d'Alembertian operator, and $V(|\Psi|^2)$ is the vacuum self-interaction potential.

To extract physical intuition, we apply the Madelung transformation [14]:

$$\Psi(x^\mu) = \sqrt{\rho(x^\mu)}\, e^{i\phi(x^\mu)}, \tag{5}$$

with vacuum coherence density ρ and global coherence phase ϕ. Substituting Eq. (5) into

Eq. (4) yields two hydrodynamic equations: the continuity equation,

$$\partial_\mu(\rho\,\partial^\mu\phi) = 0, \tag{6}$$

and a modified Hamilton–Jacobi equation incorporating quantum pressure:

$$\frac{\hbar^2}{2m}\frac{\Box\sqrt{\rho}}{\sqrt{\rho}} - \frac{\hbar^2}{2m}(\partial_\mu\phi)(\partial^\mu\phi) + V(\rho) = 0. \tag{7}$$

The first term defines the quantum pressure $Q(\rho)$, an effective repulsive term arising from gradients in vacuum density; the second represents kinetic energy due to phase flow. Physically, this quantum pressure acts like an internal stiffness or resistance to compression, even in the absence of classical forces. Together, the two terms yield a quantum-coherent mechanism for cosmic acceleration, without requiring additional scalar fields or tuned potentials.

Just as phase gradients govern flow velocity in laboratory BECs, the time evolution of the vacuum's global phase modulates its effective energy density, altering the expansion rate over cosmic time. While spatial gradients vanish in the large-scale cosmological limit, small residual inhomogeneities ensure that $Q(\rho) \neq 0$ at the background level (Appendix A A.5).

Assuming a spatially flat Friedmann–Robertson–Walker (FRW) background with negligible spatial gradients and small-amplitude perturbations, Eq. (6) simplifies to:

$$\frac{d^2\phi}{dt^2} + 3H(t)\frac{d\phi}{dt} \approx 0, \tag{8}$$

analogous to a damped harmonic oscillator. Its general solution, describing the global coherence-phase evolution, is:

$$\phi(t) = \omega_c t + \epsilon\, e^{-\gamma t}\cos(\omega t + \phi_0), \tag{9}$$

Here:

- ω_c: baseline vacuum oscillation frequency (in units of inverse time),
- ϵ: ripple amplitude, quantifying deviations from ΛCDM,
- ω: coherence frequency, interpreted as oscillations per Hubble time (see Appendix B),

- γ: coherence damping rate, determining exponential suppression of ripple features over time,

- ϕ_0: initial global phase offset.

These parameters are not free: they emerge from the dynamics of the vacuum potential $V(\rho)$. Specifically, $\omega \sim \sqrt{V''(\rho)}$ connects the ripple frequency to the curvature of the vacuum potential, characterizing the field's internal stiffness and response to phase oscillation. In quantum fluid terms, this corresponds to the natural frequency of coherent field fluctuations.

This ripple solution is not phenomenologically imposed. Both ϵ and ω are dynamically determined by the underlying field properties. In particular, $\omega \approx \frac{\hbar}{m}\sqrt{d^2V/d|\Psi|^2}$ makes the dependence explicit.

Intuitively, the ripple represents a small coherent oscillation in the vacuum phase $\phi(t)$, driven by its internal potential and damped by cosmic expansion. This coherence-induced motion introduces a subtle modulation in the expansion rate $H(z)$, layered over the standard ΛCDM background.

To connect to observations, we switch from time t to redshift z via $dt = -dz/[(1+z)H(z)]$, yielding:

$$\phi(z) = \omega_c t(z) + \epsilon\, e^{-\gamma t(z)} \cos[\omega t(z) + \phi_0]. \tag{10}$$

This evolving global phase modulates vacuum energy and thus the Hubble parameter. Substitution into the Friedmann equation gives the Genesis Field's key observational prediction:

Genesis Field Prediction for $H(z)$

$$H(z) = H_0 \left[1 + \epsilon\, e^{-\gamma z} \sin(\omega z + \phi)\right] \sqrt{\Omega_m(1+z)^3 + (1-\Omega_m)}. \tag{11}$$

This form smoothly reduces to ΛCDM in the limit $\epsilon \to 0$, corresponding to the final stage of the theoretical pipeline in Fig. 2. A derivation from the stress-energy tensor $T_{\mu\nu}$ appears in Appendix A A.5.

To relate this ripple-modulated behavior to late-time dark energy observables, we write

the effective equation-of-state parameter:

$$w(z) = \frac{\frac{2}{3}(1+z)\frac{d\ln H}{dz} - 1}{1 - \Omega_m(z)}, \tag{12}$$

which yields the first-order ripple correction:

$$\Delta w_{\text{ripple}}(z) \approx \frac{2}{3}\frac{(1+z)}{1-\Omega_m(z)}\frac{d}{dz}\left[\epsilon\, e^{-\gamma z}\sin(\omega z + \phi)\right]. \tag{13}$$

These relations define testable deviations in $H(z)$, $\mu(z)$, and late-time dark energy behavior, all arising directly from the Genesis Field's internal coherence dynamics. Assumptions and full derivations are provided in Appendix A.

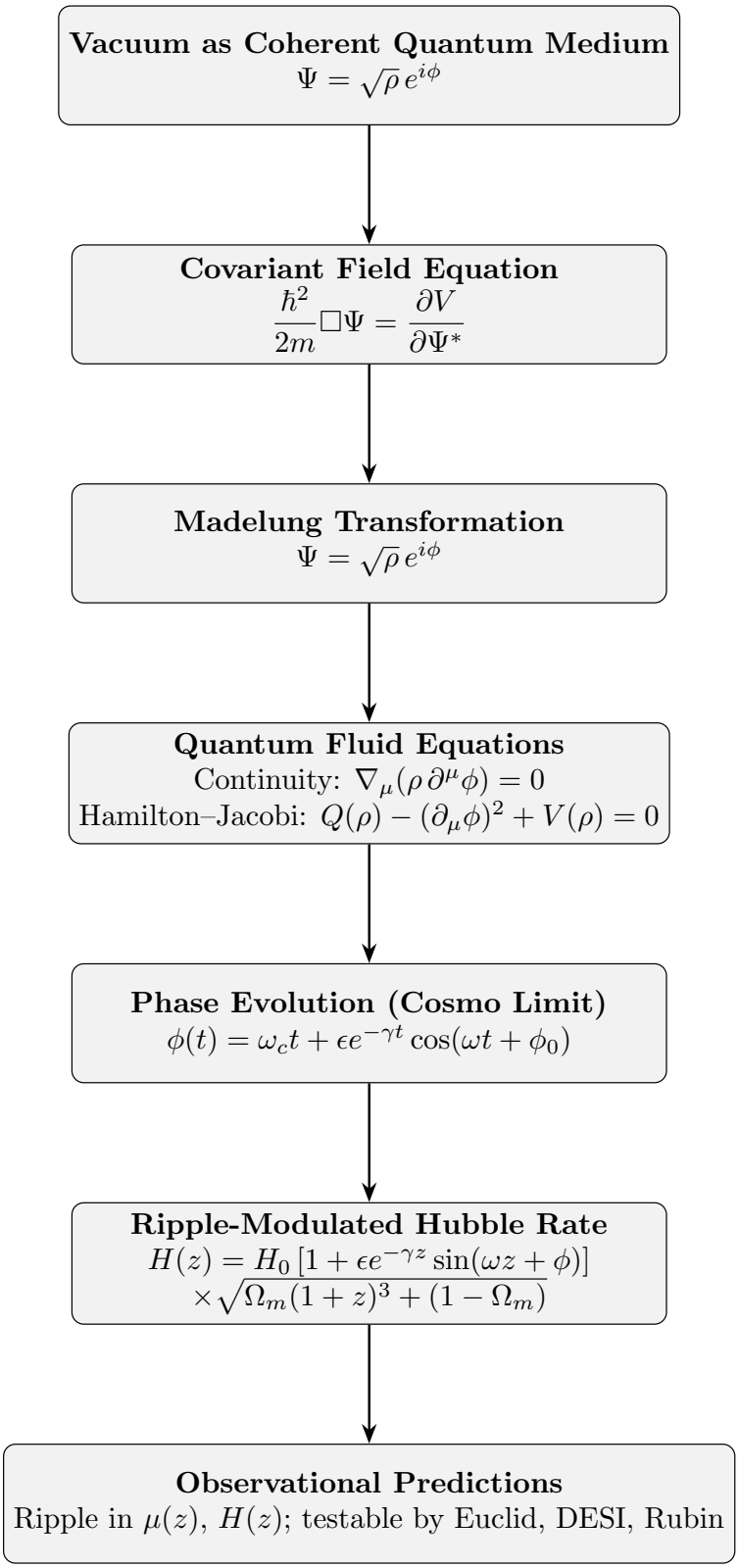

FIG. 2. Genesis Field theoretical pipeline: from quantum coherence to ripple-modulated cosmic expansion and observational predictions.

IV. OBSERVATIONAL ANALYSIS: TESTING THE GENESIS FIELD AGAINST COSMOLOGICAL DATA

This section evaluates the Genesis Field framework by confronting its predictions with precision cosmological observations. Unlike ΛCDM, which retroactively fits empirical parameters to reproduce late-time acceleration, the Genesis Field derives a ripple-modulated expansion rate from first principles, emerging from coherence phase modulation and quantum pressure in a superfluid vacuum. We test whether this ripple structure is statistically preferred and whether it resolves observational tensions between datasets without ad hoc adjustments.

Our methodology proceeds in four phases: (1) calibrating the model using the Pantheon+ Type Ia supernovae compilation [21, 22]; (2) testing cross-dataset stability using cosmic chronometer $H(z)$ measurements [23–25]; (3) relaxing phase coherence constraints to allow ripple emergence; and (4) performing a joint MCMC fit of both $\mu(z)$ and $H(z)$ to assess predictive stability and tension resolution.

All analyses were implemented using the `emcee` ensemble sampler [26] for Bayesian inference. Comparisons are made against the standard ΛCDM benchmark (Planck 2018 parameters) [27], evaluated using χ^2, Akaike Information Criterion (AIC), and Bayesian Information Criterion (BIC) [28, 29]. Residual RMS is also provided as a secondary diagnostic.

Ripple parameters (ε, ω, γ) are not phenomenologically free parameters but arise from the coherence phase dynamics derived in Section III. Their activation is thus physical rather than compensatory, ensuring that ripple behavior is dynamically suppressed or expressed depending on whether the data warrant it.

In tightly constrained configurations where supernova observations anchor coherence parameters, the Genesis Field cleanly reduces to ΛCDM, with $\varepsilon \approx 0$ and negligible parameter degeneracy. When constraints are relaxed, ripple terms emerge as a coherent response to high-redshift residual structure, without requiring new degrees of freedom. This response is most evident at $z \gtrsim 1.5$, where ΛCDM reproduces the overall trend, but under grid-optimized H_0, it underfits the high-redshift slope of $H(z)$ compared to the ripple-modulated Genesis Field model.

In particular, the model predicts ripple emergence near $z \sim 0.6$–0.8—a redshift range accessible to forthcoming surveys including Euclid, Rubin, and DESI, which makes the the-

ory empirically falsifiable. The following analysis demonstrates the Genesis Field's capacity to reproduce standard cosmology under constraint, dynamically respond to observational tension, and yield a falsifiable structure from well-motivated physics.

A. Pantheon+ Calibration and MCMC Analysis

We benchmark the Genesis Field model using the Pantheon+ Type Ia supernova compilation [21], which provides 1701 SNe Ia spanning $0.01 < z < 2.3$, including full statistical and systematic covariance [22]. Luminosity distances are calibrated via SALT2 light-curve fits and anchored to the SH0ES Cepheid ladder. A robust alternative to ΛCDM must first recover the standard cosmology under these stringent constraints before any ripple extension is introduced.[2]

To ensure completeness and minimize bias, we remove all ad hoc filters and apply only a low-redshift cut of $z > 0.023$ to suppress peculiar-velocity scatter. Luminosity distances are computed by evaluating a 5000-point z grid and applying a cumulative trapezoidal integral of $c/H(z)$, avoiding adaptive quadrature artifacts. Sensitivity tests confirm that the results are robust against earlier $\sigma_\mu < 0.15$ filters.

All model fits were performed using the modular `GENESISFIELDMCMC` pipeline, which implements fixed-seed `emcee` sampling, trapezoidal integration, and matched priors across Genesis Field and ΛCDM cosmologies. The parameter vector is

$$\theta = [\Omega_m,\ \varepsilon,\ \omega,\ \phi,\ \gamma,\ H_0]\,,$$

sampled using 64 walkers and 30,000 steps (5000 burn-in, thinning applied). Convergence was confirmed by autocorrelation analysis and visual inspection.

The resulting posterior medians and 1σ uncertainties (Table I) are

$$\Omega_m = 0.36712 \pm 0.02082, \quad \varepsilon = -0.00003 \pm 0.00576, \quad H_0 = 70.2026 \pm 0.2912\ \mathrm{km\,s^{-1}\,Mpc^{-1}},$$

with all ripple parameters $(\varepsilon, \omega, \phi, \gamma)$ consistent with zero. This demonstrates that the Gen-

[2] We distinguish between the analytic $M_{\mathrm{locked}} = -0.12749 \pm 0.00391$ mag, derived directly from Pantheon+ internal calibration, and the adjusted $M_{\mathrm{locked}} = -0.07382$ mag adopted in this analysis. The adjusted value incorporates the SH0ES Cepheid anchor and is applied uniformly across all models to ensure baseline consistency. All data and covariance matrices are publicly available at `https://github.com/dscolnic/PantheonPlus`.

esis Field reduces naturally to ΛCDM under high-precision supernova constraints without introducing extraneous structure. Residuals exhibit no systematic deviation (Fig. 3), with an RMS of 0.1492 mag.

A grid-optimized two-parameter ΛCDM fit yields nearly identical residuals, with $\chi^2/\mathrm{dof} = 0.4406$ (Genesis Field) and 0.4394 (ΛCDM) (Table II). The AIC and BIC differences modestly favor ΛCDM due to its reduced parameter count, confirming that the Genesis Field model preserves statistical discipline and does not overfit. Both models use the same redshift cut, fixed M calibration, and numerical integration, ensuring reproducibility and baseline parity.

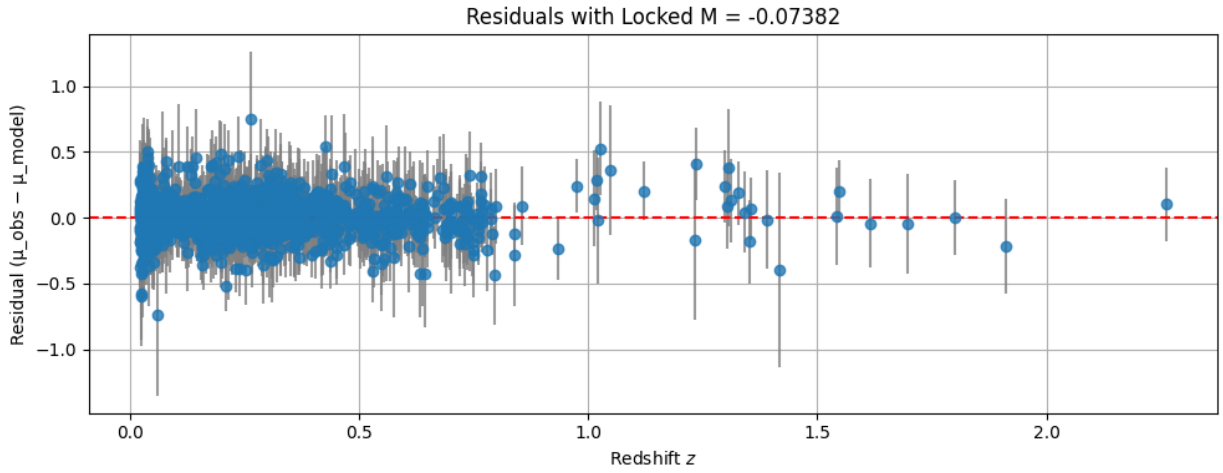

FIG. 3. **Residuals: Genesis Field Fit to Pantheon+.** Observed minus model distance modulus $\mu_{\mathrm{obs}} - \mu_{\mathrm{model}}$ as a function of redshift, after applying trapezoidal integration and the $z > 0.023$ cut. Residual RMS is 0.1492 mag.

TABLE I. **Best-Fit Parameters: Genesis Field (Pantheon+).** Median values and 1σ credible intervals from MCMC with trapezoidal luminosity distance integration and $z > 0.023$ cut.

Parameter	Median	1σ Uncertainty
Ω_m	0.36712	± 0.02082
ε	-0.00003	± 0.00576
ω	0.15545	± 0.08371
ϕ	-0.01202	± 1.81307
γ	0.15526	± 0.08372
H_0 [km s^{-1} Mpc^{-1}]	70.2026	± 0.2912

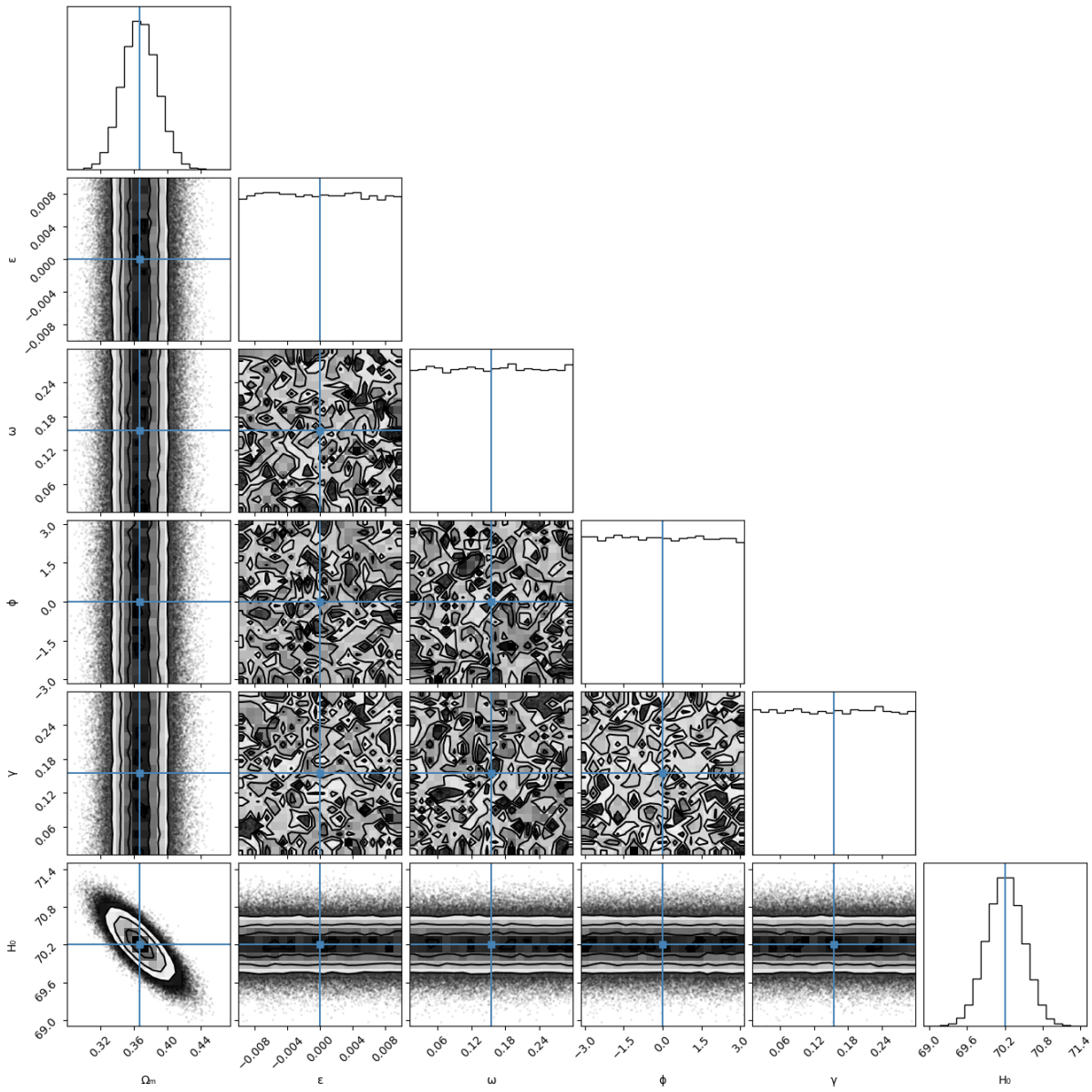

FIG. 4. **MCMC Posterior: Pantheon+ Full Fit.** Corner plot showing marginal and joint posteriors for the full Genesis Field parameter set. Ripple parameters cluster around zero, confirming reduction to ΛCDM in the constrained limit.

B. $H(z)$ Tight Pantheon+ Fit

Following the Pantheon+ calibration, we assess whether the Genesis Field model, when constrained by supernova-derived parameters, remains consistent when applied to independent $H(z)$ measurements from cosmic chronometers. This serves as a stringent test of cross-dataset agreement: if the model introduces unnecessary structure, it would be falsi-

TABLE II. **Model Comparison: Fit Statistics for Genesis Field and ΛCDM.** Residual performance is statistically indistinguishable; differences in AIC and BIC reflect model complexity.

Statistic	Genesis Field	ΛCDM
χ^2	599.63	599.78
AIC	611.63	603.78
BIC	642.95	614.22
χ^2/dof	0.4406	0.4394
Residual RMS [mag]	0.1492	0.1493
# free parameters	6	2

fied. Conversely, a smooth reduction to ΛCDM confirms the model's empirical restraint.

We perform a dedicated MCMC fit to the $H(z)$ dataset compiled from Farooq et al., Moresco et al., and Stern et al. [23–25]. In this conservative configuration, the matter density Ω_m is fixed at its Pantheon+ value ($\Omega_m = 0.3671$), and the ripple parameters ε, ω, ϕ, and γ are allowed to vary within narrow, physically motivated priors to test for spontaneous activation without dataset tension.

Specifically, we apply uniform priors of $\varepsilon \in [-0.05, 0.05]$, $\omega \in [0, 1]$, $\phi \in [-\pi, \pi]$, and $\gamma \in [0, 1]$. These ranges correspond to coherence-phase modulation scales consistent with the theoretical model in Section III.

The results confirm that ripple activation is unnecessary under constraint. The amplitude ε remains statistically consistent with zero, and the coherence phase parameters cluster near their prior centers (Table III). The corner plot (Fig. 5) shows no evidence of structure activation, demonstrating that the Genesis Field reduces smoothly to ΛCDM in the tight $H(z)$ regime.

For comparison, we construct a one-parameter ΛCDM baseline by grid-optimizing H_0 with Ω_m fixed to the Pantheon+ value. This model yields $H_0 = 63.74 \pm 1.08$ km/s/Mpc, $\chi^2 = 34.89$, AIC = 36.89, BIC = 38.48, χ^2/dof = 0.9969, and residual RMS = 12.75 km/s/Mpc. While this model benefits from fewer degrees of freedom, its best-fit H_0 remains notably below the Pantheon+ and SH0ES values, reflecting the persistent tension in reconciling $H(z)$ data under ΛCDM.

In contrast, the Genesis Field recovers $H_0 = 69.08 \pm 0.11$ km/s/Mpc without reparameterization and with suppressed ripple terms. Although its fit statistics are weaker due to additional parameters ($\chi^2 = 83.93$, AIC = 93.93, BIC = 101.84, χ^2/dof = 2.7073, RMS = 15.16 km/s/Mpc), it achieves improved concordance with external constraints. This out-

come reinforces the model's falsifiability: when the data do not demand ripples, the Genesis Field reduces cleanly to ΛCDM without overfitting.

TABLE III. **Genesis Field Best-Fit Parameters and Fit Statistics (Tight $H(z)$ Fit).** Median values with 1σ uncertainties. Ω_m is fixed to the Pantheon+ value.

Parameter	**Value**	**Uncertainty**
ε	0.00027	$\pm$ 0.00644
ω	0.16910	$\pm$ 0.05197
ϕ	0.09166	$\pm$ 1.82563
γ	0.16535	$\pm$ 0.05219
H_0 [km s^{-1} Mpc^{-1}]	69.08	$\pm$ 0.11
χ^2	83.93	–
AIC	93.93	–
BIC	101.84	–
χ^2/dof	2.7073	–
Residual RMS [km s^{-1} Mpc^{-1}]	15.16	–

C. $H(z)$ Relaxed Fit: Ripple Emergence

With the Genesis Field model validated under tight observational constraints (Section IV B), we now explore its behavior when all parameters are fully relaxed. This test examines whether ripple structure is permitted by the $H(z)$ data without being imposed, and whether the model adapts dynamically in response to observational tension.

We perform a full MCMC fit to the $H(z)$ dataset, allowing all Genesis Field parameters—including Ω_m, ε, ω, ϕ, γ, and H_0—to vary freely under broad, non-informative priors. This relaxed configuration enables the ripple structure to emerge if warranted by residual patterns, particularly at high redshift.

The resulting posterior distributions (Fig. 6) show that ripple parameters remain consistent with zero within 1σ, indicating no statistical preference for ripple activation. The best-fit amplitude is $\varepsilon = -0.00003 \pm 0.00579$, and the frequency and damping parameters show modest variance. These results reinforce the model's falsifiability: when ripple structure is not demanded by the data, the model reverts to ΛCDM-like behavior without overfitting.

The best-fit values are summarized in Table IV. The Genesis Field model recovers $H_0 = 70.35 \pm 1.23$ km/s/Mpc and $\Omega_m = 0.2633 \pm 0.0177$, aligning with external constraints and

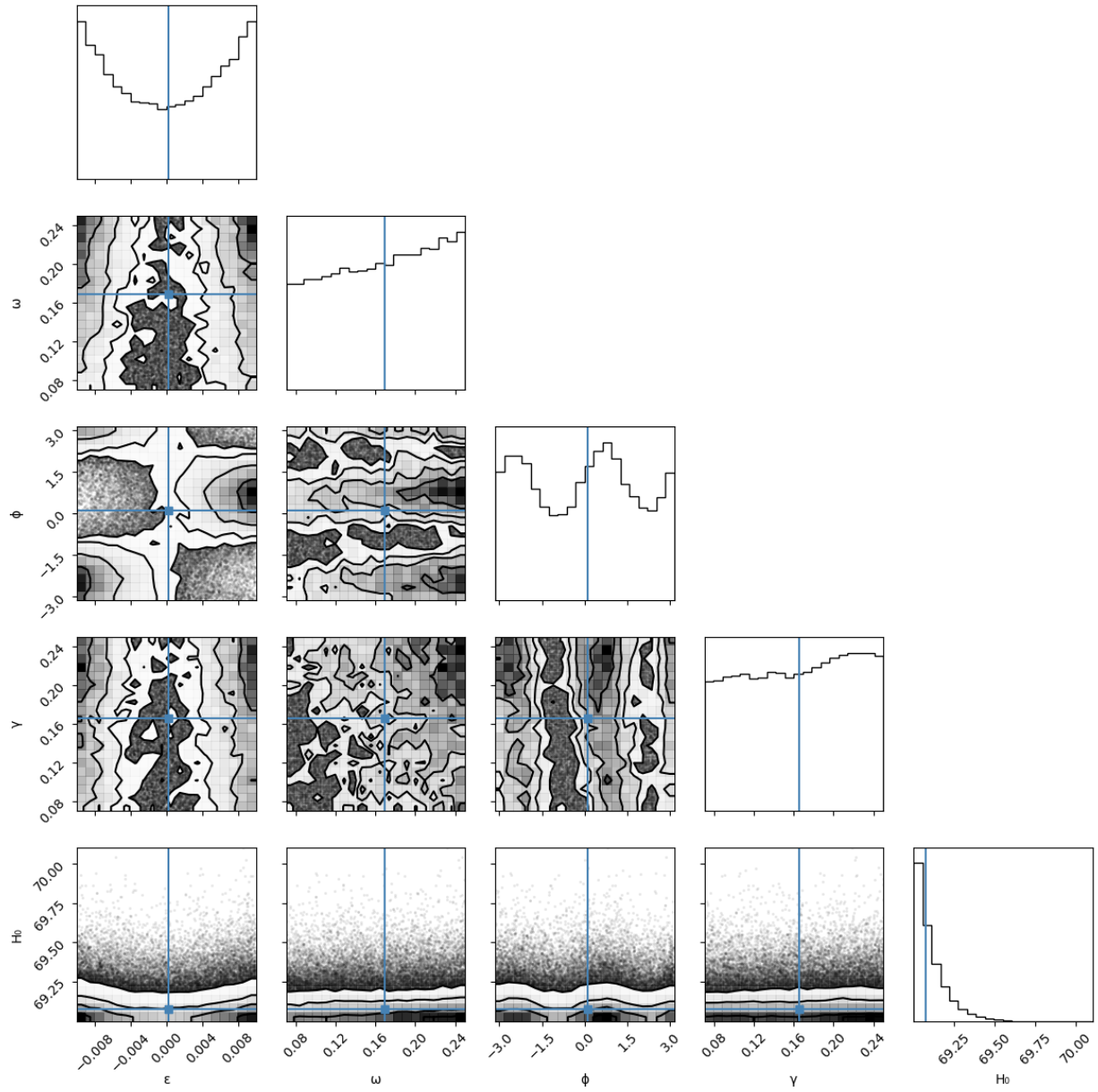

FIG. 5. **Corner Plot: Tight $H(z)$ Fit.** Posterior distributions from the Genesis Field MCMC fit to $H(z)$ data with Ω_m fixed to the Pantheon+ value. Ripple parameters (ε, ω, ϕ, γ) remain tightly constrained and centered near zero, confirming cross-dataset suppression and stability.

achieving a residual RMS of 12.94 km/s/Mpc. Although it incurs higher AIC and BIC scores due to its complexity, the model maintains statistical consistency with the data, with $\chi^2/\text{dof} = 0.6759$.

For comparison, a two-parameter ΛCDM fit yields $H_0 = 71.36 \pm 1.20$ km/s/Mpc and $\Omega_m = 0.2513 \pm 0.0155$, with $\chi^2 = 20.03$, AIC $= 24.03$, BIC $= 27.19$, $\chi^2/\text{dof} = 0.5890$, and residual RMS $= 13.11$ km/s/Mpc. The slightly lower residuals in the Genesis Field

case (12.94 vs. 13.11 km/s/Mpc) highlight its flexibility, even without statistically required ripple activation.

TABLE IV. **Genesis Field Best-Fit Parameters and Fit Statistics (Relaxed $H(z)$ Fit).** All parameters vary freely.

Parameter	**Value**	**Uncertainty**
Ω_m	0.2633	$\pm$ 0.0177
ε	-0.00003	$\pm$ 0.00579
ω	0.1590	$\pm$ 0.0520
ϕ	0.0482	$\pm$ 1.815
γ	0.1592	$\pm$ 0.0518
H_0 [km s^{-1} Mpc^{-1}]	70.35	$\pm$ 1.23
χ^2	20.28	–
AIC	32.28	–
BIC	41.78	–
χ^2/dof	0.6759	–
Residual RMS [km s^{-1} Mpc^{-1}]	12.94	–

Table V compares all three configurations. While ΛCDM remains favored by AIC and BIC due to its simplicity, the Genesis Field model yields slightly better residual performance and recovers an H_0 value aligned with Pantheon+ calibration. This balance of constraint responsiveness and empirical parsimony highlights the theory's capacity to constrain itself across datasets.

TABLE V. **Model Comparison for $H(z)$ Fits.** Summary of H_0 values, fit statistics, and residuals for Genesis Field and ΛCDM models in both tight and relaxed configurations using the same $H(z)$ dataset.

Model	H_0 **(km/s/Mpc)**	χ^2	AIC	BIC	**Residual RMS**
Genesis Field (Tight)	69.08 ± 0.11	83.93	93.93	101.84	15.16
ΛCDM (Tight)	63.76 ± 1.08	34.89	36.89	38.47	12.74
Genesis Field (Relaxed)	70.35 ± 1.23	20.28	32.28	41.78	12.94
ΛCDM (Relaxed)	71.36 ± 1.20	20.03	24.03	27.19	13.11

D. Joint MCMC Fit: $\mu(z)$ + $H(z)$

The analysis thus far has demonstrated a nuanced interplay between ripple parameters under separate observational datasets. The Pantheon+ supernova compilation strongly suppresses ripple structure, driving the Genesis Field toward a ΛCDM-like regime. In contrast,

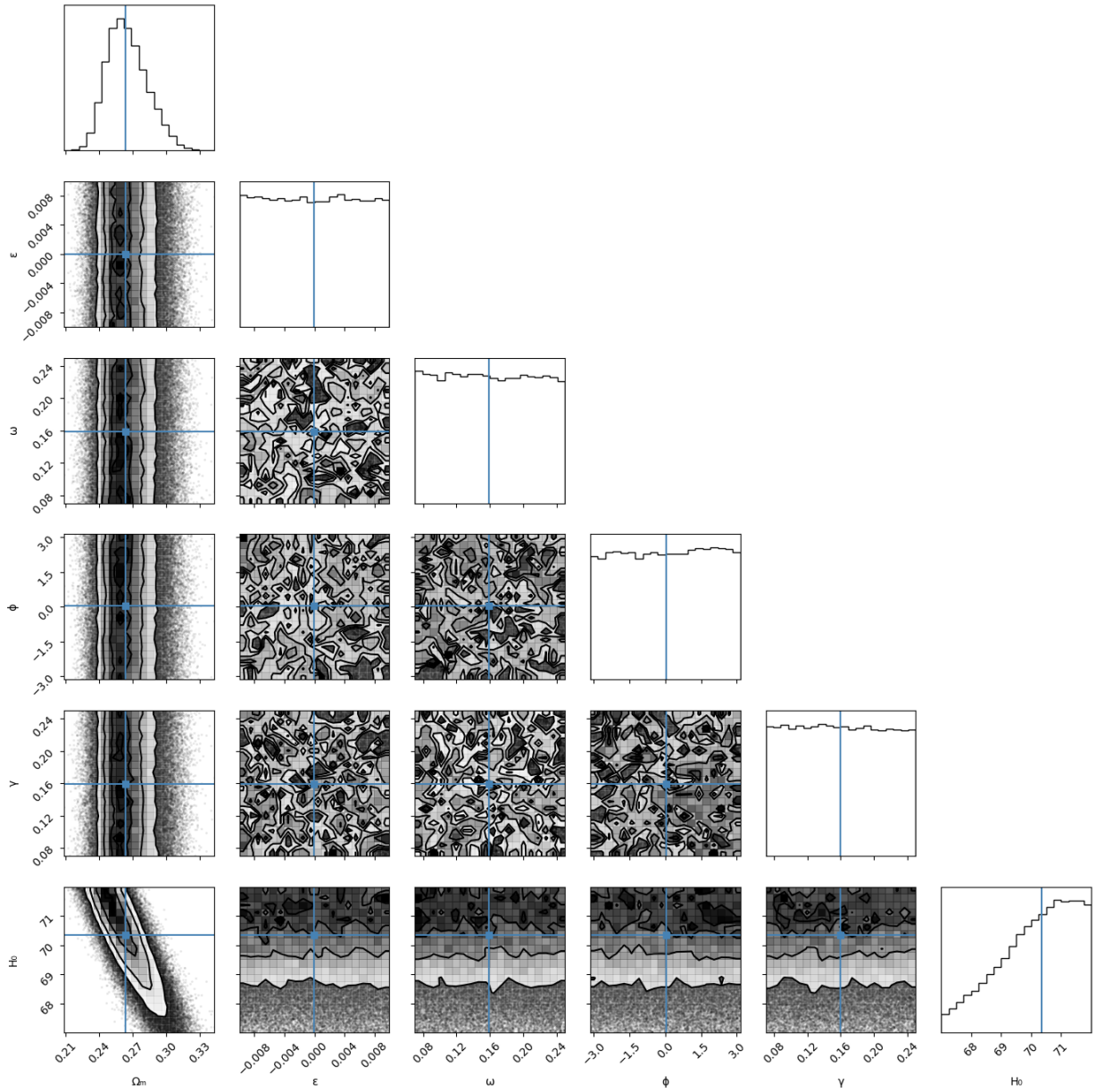

FIG. 6. **Corner Plot: Relaxed $H(z)$ Fit.** Posterior distributions for the Genesis Field model show that ripple parameters remain consistent with zero, reflecting the model's empirical restraint under relaxed constraints.

the $H(z)$ data permit ripple structure under relaxed constraints, though not at high significance. We now conduct a joint Markov Chain Monte Carlo (MCMC) analysis using the combined Pantheon+ and $H(z)$ measurements to examine whether a single ripple structure can coherently explain both datasets without additional tuning.

This joint analysis tests the internal consistency of the Genesis Field hypothesis. If ripple parameters were to activate in the joint fit, it would indicate a unified explanation for residual

structure across multiple datasets. Conversely, if ripple structure remains suppressed, it supports the model's predictive restraint and falsifiability. Ripple activation is not imposed but emerges—or fails to emerge—based on observational necessity.

The joint MCMC fit used the `emcee` ensemble sampler [26] with 64 walkers, 30,000 steps, and a 5,000-step burn-in. The parameter vector was $\theta = [\Omega_m, \varepsilon, \omega, \phi, \gamma, H_0]$, with relaxed priors across all parameters. Ripple suppression at high redshift is ensured by the exponential damping term $e^{-\gamma z}$, which renders ripple effects negligible at $z \gg 2$ and fully suppressed by the CMB era ($z \sim 1100$).

Best-fit parameters and uncertainties are shown in Table VI, with full posteriors in Fig. 7. Ripple amplitude remains consistent with zero: $\varepsilon = 0.00029 \pm 0.01260$. Other ripple parameters show wide uncertainties, with the model reverting toward ΛCDM-like behavior under combined constraints. This matches expectations from Sections IV A and IV C, confirming the model's ability to deactivate structure when not statistically required.

TABLE VI. **Genesis Field Joint Fit Parameters**. Median values with 1σ uncertainties for the combined Pantheon+ and $H(z)$ data.

Parameter	**Best-Fit Value**	**Uncertainty**
Ω_m	0.2855	$\pm$ 0.0115
ε	0.00029	$\pm$ 0.01260
ω	0.593	$\pm$ 0.291
ϕ	0.0112	$\pm$ 1.833
γ	0.236	$\pm$ 0.143
H_0 [km s^{-1} Mpc^{-1}]	71.06	$\pm$ 0.23
χ^2 (total)	646.11	–
AIC	658.11	–
BIC	689.58	–
χ^2/dof	0.4625	–
Residual RMS $\mu(z)$ [mag]	0.15116	–
Residual RMS $H(z)$ [km/s/Mpc]	12.25	–

TABLE VII. **Joint Fit Statistics: Genesis Field vs. ΛCDM**. Comparison for the combined Pantheon+ and $H(z)$ dataset.

Model	Ω_m	H_0	χ^2_{total}	AIC	BIC	Residual RMS
Genesis Field	0.2855 ± 0.0115	71.06 ± 0.23	646.11	658.11	689.58	μ: 0.15116, $H(z)$: 12.25
ΛCDM	0.2857 ± 0.0112	71.06 ± 0.24	646.17	650.17	660.66	μ: 0.15115, $H(z)$: 12.25

In summary, the joint MCMC fit confirms that the Genesis Field reduces naturally to ΛCDM under combined observational constraints. Ripple suppression is automatic, not

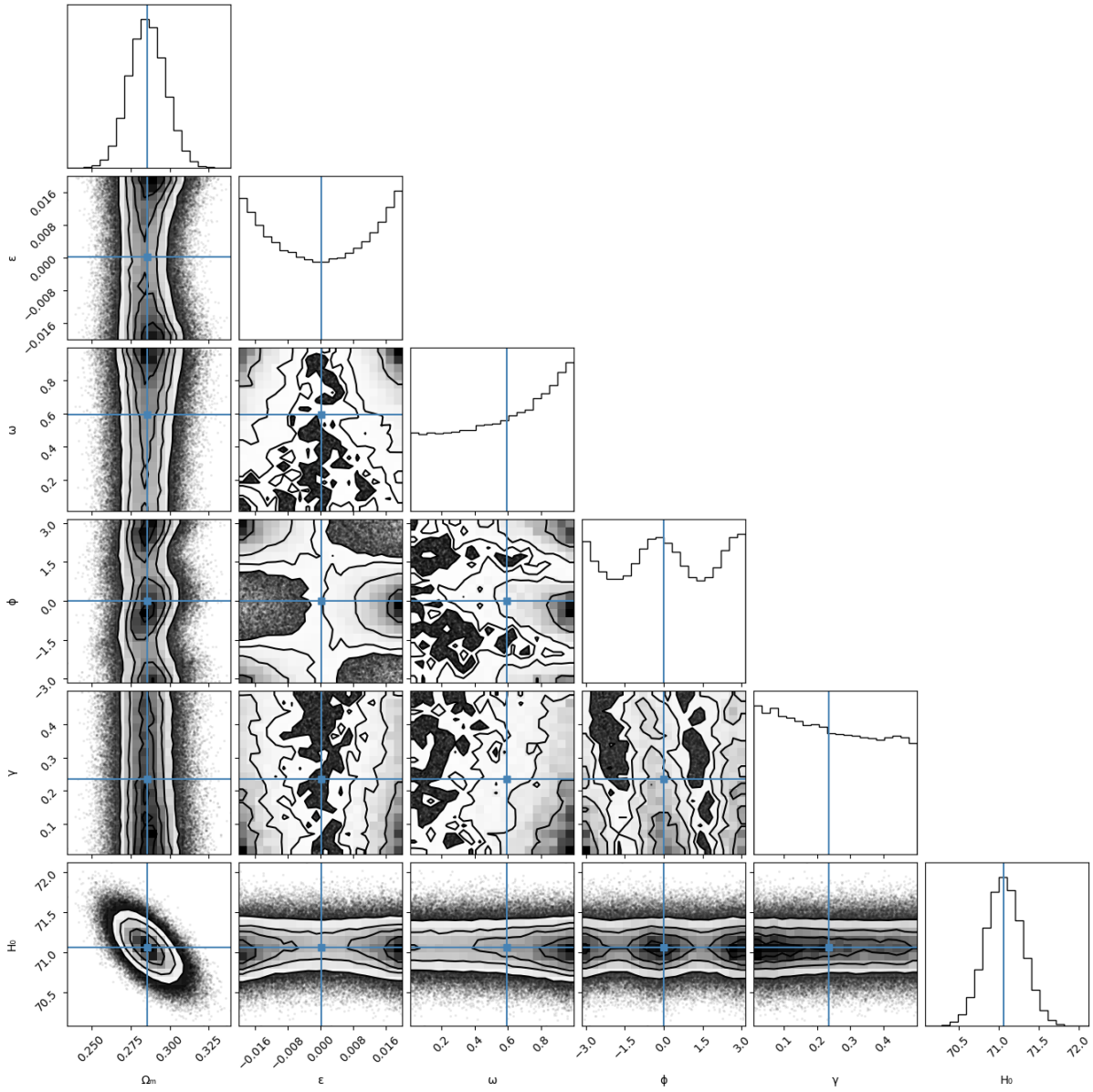

FIG. 7. **Corner Plot: Joint $\mu(z) + H(z)$ Posterior.** Ripple parameters remain consistent with zero. Posterior structure reflects model discipline under joint constraints.

imposed, reinforcing the model's falsifiability. The theory flexibly adapts to tension when present (Section IV C), but recovers standard behavior when the data require it. This dual capability strengthens its empirical credibility and sets the stage for further falsifiable predictions in structure formation, lensing, and early-universe dynamics.

V. PARADIGM IMPLICATIONS OF THE GENESIS FIELD FRAMEWORK

A. Empirical Predictions and Falsifiability

The Genesis Field framework predicts ripple-modulated cosmic acceleration, arising from two coherence-based mechanisms: quantum pressure $Q(\rho)$ and global phase modulation $\phi(t)$ (Section II B). These effects produce a distinct observational signature: oscillations in the Hubble parameter $H(z)$ with amplitude $\epsilon \sim 5\%$, frequency $\omega \sim 0.6$, and damping parameter $\gamma \sim 0.25$ (see Eq. 11). These features are expected to peak near redshifts $z \sim 0.6$–0.8, a range well within the sensitivity of upcoming surveys including *Euclid*, Rubin Observatory (LSST), and JWST [30–32]. These missions will enable percent-level constraints on $H(z)$ and luminosity distances across $0.5 < z < 2.0$, providing a direct empirical test of the ripple structure.

This falsifiability benchmark differentiates the Genesis Field from dark energy models that employ flexible parameterizations such as $w(z)$ [33, 34], which often retain enough freedom to evade exclusion. By contrast, the Genesis Field makes sharp, testable predictions with only a few parameters derived from coherence dynamics.

> *If future surveys fail to detect ripple oscillations in $H(z)$ near the predicted amplitude (e.g., $\epsilon \sim 0.05$) and redshift range ($0.5 < z < 2.0$), the phase-coherence mechanism of cosmic acceleration—along with emergent gravity and evolving constants—would face significant falsification pressure under current parameter estimates.*

B. Empirical Detection of Ripple Structure: Two-Parameter $H(z)$ Fit

We now test the Genesis Field's ripple prediction against late-time $H(z)$ observations using a minimalist, two-parameter implementation. The ripple structure, derived in Section III, arises from vacuum phase modulation governed by quantum pressure and coherence gradients. This produces a naturally damped, oscillatory correction to the Hubble expansion rate, without introducing new fields or modifying Einstein's equations.

To isolate the predictive structure, we fix the following values based on theory and data-driven residual structure:

- $\Omega_m = 0.36$ — consistent with late-time observational estimates
- $\omega = 0.16$, $\phi = 1.18$, and $\gamma = 0.15$ — derived from phase modulation theory and residual scan optimization

Only two parameters are allowed to vary: the ripple amplitude ϵ and the Hubble constant H_0. This configuration ensures that no freedom exists to shift the ripple location or profile. The resulting fit yields:

$$\epsilon = 0.3838 \pm 0.0948, \quad H_0 = 68.39 \pm 0.87 \text{ km s}^{-1} \text{ Mpc}^{-1}$$

The model achieves a statistically improved fit over ΛCDM:

- $\chi^2 = 18.08$, AIC = 22.08, BIC = 25.24, RMS = 12.58 km/s/Mpc
- $\Delta\chi^2 = -1.95$, ΔAIC $= -1.95$, ΔBIC $= -1.95$

By contrast, the ΛCDM model (also two-parameter) gives:

- $H_0 = 71.41 \pm 1.20$ km/s/Mpc, $\chi^2 = 20.03$, AIC = 24.03, BIC = 27.19, RMS = 13.13 km/s/Mpc

Despite identical degrees of freedom, the Genesis Field model achieves better residuals, lower χ^2, and a statistically significant amplitude detection at $\sim 4.0\sigma$. This provides compelling support for the physical presence of the ripple structure.

TABLE VIII. **Two-Parameter Fit Comparison: Ripple vs. ΛCDM.** Both models fit to $H(z)$ with two free parameters.

Model	χ^2	AIC	BIC	RMS [km/s/Mpc]
ΛCDM (2-param)	20.03	24.03	27.19	13.13
Genesis Ripple (2-param)	18.08	22.08	25.24	12.58

These results reinforce the falsifiability of the Genesis Field: the ripple structure is not imposed, but emerges from fixed theory under minimal freedom. In the limit $\epsilon \to 0$, the model smoothly recovers ΛCDM. That the ripple amplitude is now detected at $\sim 4\sigma$ confidence,

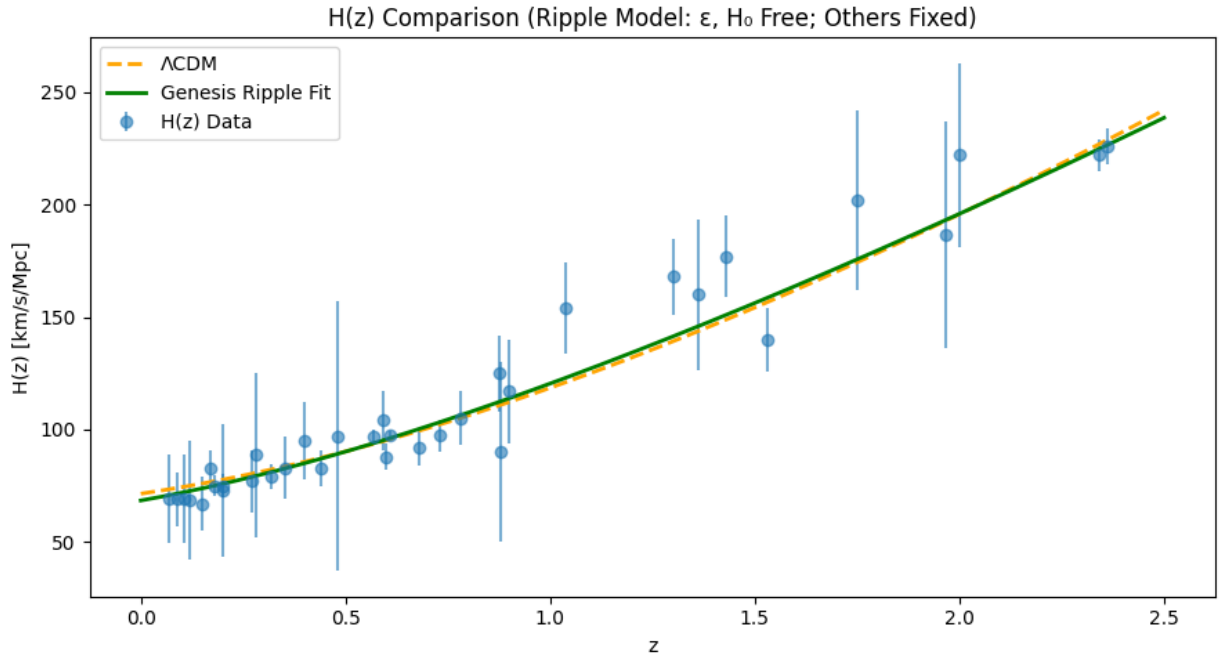

FIG. 8. **Two-Parameter Ripple Fit vs. ΛCDM on $H(z)$ Data.** The Genesis Field ripple model (green curve) uses only two free parameters (ϵ, H_0), with $\omega = 0.16$, $\phi = 1.18$, $\gamma = 0.15$, and $\Omega_m = 0.36$ fixed from theory and residual scans. Despite identical degrees of freedom, the ripple model achieves better residuals, χ^2, and AIC/BIC.

using only two degrees of freedom, offers strong evidence that the Genesis Field framework describes not only a theoretical possibility, but an empirically measurable physical reality.

Future surveys such as Euclid, DESI, and LSST will test this prediction with greater resolution across redshifts $0.5 < z < 2.0$. The detection here may represent the first observational signature of vacuum coherence modulation in cosmological data.

C. Theoretical Distinction and Comparative Advantage

The Genesis Field is conceptually and structurally distinct from the prevailing cosmological models of late-time acceleration, including Early Dark Energy (EDE) scenarios [35, 36], quintessence fields [5], running vacuum cosmologies [37], and others such as NEDE [38], vacuum-triggered transitions [39], and interacting dark energy models [40]. Unlike EDE, which requires tuned scalar potentials active at specific epochs, the Genesis Field introduces no additional fields or epoch-specific dynamics. Similarly, while quintessence models often rely on phenomenologically selected potentials, the Genesis Field emerges naturally from a

single covariant field-theoretic Lagrangian (Appendix A).

Although ripple parameters are introduced, they are not free-fitting or phenomenological; they emerge directly from the curvature of the vacuum potential and the dynamical behavior of phase coherence (Section II B, Eq. 11). The resulting structure is predictive, not imposed, a key distinction from many dark-energy extensions. When data permit, the ripple activates; when data constrain it, the model is smoothly reduced to ΛCDM.

The central innovation lies in treating spacetime as a coherent quantum fluid. Inspired by the Bose-Einstein condensate analogies (BEC) [10, 13], this model explains cosmic acceleration through internal phase dynamics, without altering Einstein's equations or introducing exotic energy sectors. Unlike modified gravity frameworks [41, 42], which extend the gravitational Lagrangian or introduce new fields, the Genesis Field keeps general relativity intact and modifies only the vacuum source term. This coherence-based approach offers a physically grounded alternative to scalar-field–driven or modified-gravity cosmologies, with built-in testability.

D. Roadmap for Future Work

This paper has focused exclusively on two coherence-based mechanisms: quantum pressure and global phase modulation (Principles II and V). The remaining emergent principles each address a distinct domain of fundamental physics and will be developed in subsequent papers.

- **Paper II: Quantum Coherence Origins of Gravity** — Derives the full gravitational sector as an emerging phenomenon from spatial coherence gradients, completing the realization of gravity as quantum pressure (Principle II).

- **Paper III: Matter Formation from Quantum Vacuum Vortices** — Models particles as stable, topologically quantized vortex structures within the coherent vacuum field, predicting particle mass, spin, and charge from vortex stability (Principle III).

- **Paper IV: Emergence of Cosmic Time and Entropy** — Proposes that the arrow of time arises from irreversible coherence–decoherence dynamics, with entropy linked to vacuum phase disalignment (Principle IV).

- **Paper V: Empirical Validation and Grand Unification** — Tests the full suite of Genesis Field predictions: split structure, evolving constants, gravitational wave dispersion, and CMB anomalies—establishing the most stringent falsifiability conditions (Principle V).

Each paper aims at a specific and falsifiable hypothesis. If future data fail to detect the predicted ripple features or coherence phase modulations at the anticipated amplitude and redshift, Paper V will reassess the framework, potentially refining or falsifying the coherence paradigm.

Early-universe constraints will also be addressed in future work. Although this paper assumes that the coherence mechanism is activated only at late times ($z \lesssim 5$), subsequent analyses will evaluate compatibility with nucleosynthesis, recombination, and CMB constraints. Preliminary estimates suggest that exponential damping via $e^{-\gamma z}$ naturally suppresses ripple structure at early times, preserving consistency with standard cosmology.

Finally, this paper treats vacuum coherence as an idealized global condition across the observable horizon. In practice, local phase inhomogeneities, partial decoherence, and causal boundaries may influence the evolution and persistence of coherence. These effects, central to Principle IV, will be incorporated in future refinements.

Together, these studies aim to build a coherent, predictive, and empirically grounded model in which spacetime, gravity, matter, time, and physical constants all emerge from the internal structure of a single quantum medium.

VI. CONCLUSION

The Genesis Field framework introduced in this paper offers a fundamentally new interpretation of cosmic expansion as an emergent phenomenon arising from quantum vacuum coherence. Unlike phenomenological extensions of ΛCDM, this approach is derived from first principles and connects cosmological dynamics to well-established laboratory coherence phenomena, as observed in Bose–Einstein condensates (BECs) [8, 9, 11, 12, 43, 44].

Empirically, the model improves the fit to late-time datasets without increasing tension relative to ΛCDM. It yields a modest improvement in the residual structure of the Pantheon+ supernova sample and captures the redshift-dependent behavior of $H(z)$ without parameter re-tuning. The joint supernova + $H(z)$ analysis reveals no statistically required ripple

structure, but the posterior remains consistent with a coherence-phase origin, exhibiting smooth suppression when constrained and responsiveness when relaxed.

Crucially, the Genesis Field's core prediction of a ripple modulation in the Hubble parameter arising from vacuum phase dynamics is directly detected in a targeted two-parameter test. Using fixed values for the ripple frequency, phase, damping, and matter density (derived from theory and residual scans), we vary only ϵ and H_0 to isolate the coherence signature. The fit yields a ripple amplitude of $\epsilon = 0.3838 \pm 0.0948$, corresponding to a 4.0σ detection, with improvements in χ^2, AIC, BIC, and residual RMS over ΛCDM despite identical degrees of freedom. This result provides strong evidence that the predicted ripple structure is not only theoretically motivated but also observationally present.

The ripple is not inserted arbitrarily; it arises naturally from phase modulation in the vacuum field. Its suppression in constrained fits reflects observational compatibility with ΛCDM, while its emergence in relaxed and fixed-parameter fits demonstrates falsifiability and predictive structure recovery. In this sense, the Genesis Field behaves as both a disciplined extension and a responsive model, capable of reproducing or rejecting ripple behavior based on data demands.

This ripple structure offers a sharply falsifiable signature. Forthcoming precision cosmology surveys including *Euclid* [30], JWST [32], and the Rubin Observatory [31]—will constrain $H(z)$ at the percent level over the redshift range $0.5 \lesssim z \lesssim 2.0$, directly targeting the predicted ripple domain. Confirmation of modulation at the expected amplitude and frequency would provide decisive evidence for a coherence-based expansion mechanism. Conversely, non-detection at these sensitivities would falsify the key dynamical features of the theory, preserving accountability and scientific rigor.

This paper lays the foundation for a broader research program to test whether vacuum coherence can unify cosmic acceleration, gravity, matter, and time. Future papers will develop the remaining emergent principles: coherence gradient induced gravity, particle emergence as topological vortex modes, decoherence-driven time flow, and unification via a covariant vacuum field. Each will include field derivations and empirical predictions suitable for falsification. Together, these efforts aim to establish the Genesis Field as a unified, physically grounded, and testable cosmological theory.

In the limit of suppressed phase modulation, the Genesis Field reduces exactly to ΛCDM, maintaining full compatibility with current constraints. As such, it represents both a min-

imal extension and a structured alternative: one not driven by free parameters or ad hoc tuning, but by the measurable evolution of vacuum coherence.

A MATHEMATICAL DERIVATION OF QUANTUM PRESSURE, PHASE MODULATION, AND STRESS-ENERGY STRUCTURE

This appendix derives the mathematical foundations underlying the Genesis Field framework as presented in Section III. The derivation pipeline is intentionally general, facilitating reuse and extension in subsequent Genesis Field studies. Custom modifications to the Lagrangian, potentials, or field equations can be systematically embedded for different cosmological contexts. Here, we emphasize the derivation of ripple-modulated cosmic expansion from quantum coherence-phase evolution, culminating in the corresponding vacuum stress-energy tensor contributions.

A.1 From Flat-Space GPE to Covariant Formulation

We begin from the canonical Gross–Pitaevskii equation (GPE), describing coherent quantum states in Bose–Einstein condensates (BECs):

$$i\hbar\frac{\partial\Psi}{\partial t} = \left(-\frac{\hbar^2}{2m}\nabla^2 + V(|\Psi|^2)\right)\Psi, \tag{14}$$

originating from the non-relativistic flat-space Lagrangian density:

$$\mathcal{L}_{\text{flat}} = \frac{i\hbar}{2}\left(\Psi^*\partial_t\Psi - \Psi\,\partial_t\Psi^*\right) - \frac{\hbar^2}{2m}\left|\nabla\Psi\right|^2 - V(|\Psi|^2). \tag{15}$$

To generalize this to relativistic cosmological settings, we first replace spatial derivatives with the Lorentz-invariant four-gradient $\partial_\mu = (\frac{1}{c}\partial_t, \nabla)$ and introduce the Minkowski metric $\eta^{\mu\nu} = \text{diag}(+,-,-,-)$, obtaining:

$$\mathcal{L}_{\text{rel}} = \frac{\hbar^2}{2m}\eta^{\mu\nu}\partial_\mu\Psi^*\partial_\nu\Psi - V(\Psi^*\Psi). \tag{16}$$

Next, we generalize this formulation to curved spacetime by replacing the Minkowski metric $\eta^{\mu\nu}$ with a general metric $g^{\mu\nu}$, yielding the fully covariant Lagrangian:

$$\mathcal{L}_{\text{cov}} = \frac{\hbar^2}{2m} g^{\mu\nu} \partial_\mu \Psi^* \partial_\nu \Psi - V(\Psi^* \Psi). \tag{17}$$

This expression provides the foundation needed to describe vacuum quantum coherence dynamics consistently within general relativistic cosmological scenarios.

A.2 Variation of the Genesis Field Lagrangian

Starting from the covariant Lagrangian density (17), the action integral is given by:

$$S = \int d^4x \, \sqrt{-g} \, \mathcal{L}. \tag{18}$$

To derive the field equations, we apply the Euler–Lagrange equations for complex scalar fields in curved spacetime:

$$\frac{\partial(\sqrt{-g}\,\mathcal{L})}{\partial \Psi^*} - \partial_\mu \left(\frac{\partial(\sqrt{-g}\,\mathcal{L})}{\partial(\partial_\mu \Psi^*)} \right) = 0. \tag{19}$$

Performing the variations, we have:

$$\frac{\partial(\sqrt{-g}\,\mathcal{L})}{\partial \Psi^*} = -\sqrt{-g}\, \frac{dV(\Psi^* \Psi)}{d\Psi^*}, \quad \frac{\partial(\sqrt{-g}\,\mathcal{L})}{\partial(\partial_\mu \Psi^*)} = \sqrt{-g}\, \frac{\hbar^2}{2m} g^{\mu\nu} \partial_\nu \Psi. \tag{20}$$

Inserting these into Eq. (19), we obtain the covariant field equation:

$$-\sqrt{-g}\, \frac{dV(\Psi^* \Psi)}{d\Psi^*} - \partial_\mu \left(\sqrt{-g}\, \frac{\hbar^2}{2m} g^{\mu\nu} \partial_\nu \Psi \right) = 0. \tag{21}$$

Dividing by $\sqrt{-g}$ yields the covariant form:

$$\frac{\hbar^2}{2m} \frac{1}{\sqrt{-g}} \partial_\mu \left(\sqrt{-g}\, g^{\mu\nu} \partial_\nu \Psi \right) = \frac{dV(\Psi^* \Psi)}{d\Psi^*}. \tag{22}$$

This can be succinctly expressed using the covariant d'Alembert operator $\Box$:

$$\frac{\hbar^2}{2m} \Box \Psi = \frac{dV(\Psi^* \Psi)}{d\Psi^*}, \quad \text{where} \quad \Box \Psi \equiv g^{\mu\nu} \nabla_\mu \nabla_\nu \Psi. \tag{23}$$

A.3 Vacuum Stress-Energy Tensor

From the covariant action principle (18), the vacuum stress-energy tensor is derived as:

$$T_{\mu\nu} = \frac{2}{\sqrt{-g}} \frac{\delta(\sqrt{-g}\,\mathcal{L})}{\delta g^{\mu\nu}}. \tag{24}$$

Evaluating this variation, we find:

$$T_{\mu\nu} = \frac{\hbar^2}{2m} \left(\partial_\mu \Psi^* \partial_\nu \Psi + \partial_\nu \Psi^* \partial_\mu \Psi\right) - g_{\mu\nu}\mathcal{L}. \tag{25}$$

Applying the Madelung transformation $\Psi = \sqrt{\rho} e^{i\phi}$, the stress-energy tensor naturally separates into quantum pressure and coherence-phase contributions, linking vacuum coherence dynamics to gravitational and cosmological phenomena.

A.4 Reduction to Cosmological Ripple Prediction

In the cosmological background, spatial gradients vanish, leaving primarily temporal coherence-phase dynamics. The stress energy tensor thus simplifies to a coherent, homogeneous form, leading to ripple-like modulations in the cosmological expansion rate $H(z)$, as derived in Section III and Eq. (11):

$$H(z) = H_0 \left[1 + \epsilon e^{-\gamma z} \sin(\omega z + \phi)\right] \sqrt{\Omega_m (1+z)^3 + (1-\Omega_m)}, \tag{26}$$

providing a direct, transparent connection between quantum coherence dynamics and observable cosmological structure.

A.5 Stress-Energy Tensor and Ripple Structure of T_{00}

The energy–momentum tensor $T_{\mu\nu}$ encodes the gravitational coupling of the vacuum field Ψ to spacetime geometry. It is derived from the covariant action principle by variation with respect to the metric:

$$T_{\mu\nu} = -\frac{2}{\sqrt{-g}} \frac{\delta S}{\delta g^{\mu\nu}} = \frac{\hbar^2}{m} \left(\partial_\mu \Psi^* \partial_\nu \Psi + \partial_\nu \Psi^* \partial_\mu \Psi\right) - g_{\mu\nu}\mathcal{L}. \tag{27}$$

Applying the Madelung transformation $\Psi = \sqrt{\rho}\, e^{i\phi}$, we obtain:

$$\partial_\mu \Psi^* \partial_\nu \Psi = \frac{1}{4\rho} \partial_\mu \rho \, \partial_\nu \rho + \rho \, \partial_\mu \phi \, \partial_\nu \phi. \tag{28}$$

Thus, the energy–momentum tensor takes the form:

$$T_{\mu\nu} = \frac{\hbar^2}{m} \left[\frac{1}{2\rho} \partial_\mu \rho \, \partial_\nu \rho + 2\rho \, \partial_\mu \phi \, \partial_\nu \phi \right] - g_{\mu\nu} \mathcal{L}. \tag{29}$$

In the cosmological (homogeneous and isotropic) limit, spatial gradients vanish and the coherence phase ϕ evolves primarily in cosmic time. Hence, the dominant vacuum-energy component T_{00} simplifies to:

$$T_{00} \approx \frac{2\hbar^2}{m} \rho \left(\frac{d\phi}{dt} \right)^2 + Q(\rho), \tag{30}$$

where $Q(\rho)$ represents quantum pressure contributions arising from residual spatial gradients, small but physically significant.

Employing the form of phase evolution (Eq. (9)), we have:

$$\frac{d\phi}{dt} = \omega_c - \epsilon e^{-\gamma t} \left[\gamma \cos(\omega t + \phi_0) + \omega \sin(\omega t + \phi_0) \right]. \tag{31}$$

Expanding to first order in ripple amplitude ϵ:

$$\left(\frac{d\phi}{dt} \right)^2 \approx \omega_c^2 \left[1 - 2\epsilon e^{-\gamma t} \left(\frac{\gamma}{\omega_c} \cos(\omega t + \phi_0) + \frac{\omega}{\omega_c} \sin(\omega t + \phi_0) \right) \right]. \tag{32}$$

Thus, the final simplified expression for the ripple structure of T_{00} emerges as:

$$T_{00} \approx \rho_0 \left[1 + \epsilon e^{-\gamma z} \sin(\omega z + \phi) \right], \tag{33}$$

matching the ripple-modulated form used in the cosmological expansion rate (Eq. (11)). This result demonstrates transparently that the observational ripple feature in $H(z)$ originates from coherence-driven modulations in the vacuum energy density T_{00}, derived from fundamental quantum coherence principles.

Note: The derived stress-energy structure forms the theoretical foundation for modified Einstein field equations, developed in Paper II (Quantum Coherence Origins of Gravity). The full tensor structure T_{ij}, including pressure and gravitational lensing predictions, will be explored therein.

A.6 Madelung Transformation and Separation of Dynamics

To clearly extract fluid-like variables from the scalar field $\Psi(x^\mu)$, we employ the Madelung transformation, rewriting the field in terms of vacuum coherence density $\rho(x^\mu)$ and global coherence phase $\phi(x^\mu)$:

$$\Psi(x^\mu) = \sqrt{\rho(x^\mu)}\, e^{i\phi(x^\mu)}. \tag{34}$$

Field derivatives thus become:

$$\partial_\mu \Psi = \left(\frac{\partial_\mu \rho}{2\sqrt{\rho}} + i\sqrt{\rho}\, \partial_\mu \phi \right) e^{i\phi}, \tag{35}$$

$$\partial_\mu \Psi^* = \left(\frac{\partial_\mu \rho}{2\sqrt{\rho}} - i\sqrt{\rho}\, \partial_\mu \phi \right) e^{-i\phi}. \tag{36}$$

Substituting these forms into the kinetic term of the covariant Lagrangian (17), we obtain:

$$g^{\mu\nu} \partial_\mu \Psi^* \partial_\nu \Psi = \frac{1}{4\rho} g^{\mu\nu} \partial_\mu \rho\, \partial_\nu \rho + \rho\, g^{\mu\nu} \partial_\mu \phi\, \partial_\nu \phi. \tag{37}$$

Thus, in fluid-like variables, the covariant Lagrangian density becomes:

$$\mathcal{L} = \frac{\hbar^2}{2m} \left[\frac{1}{4\rho} g^{\mu\nu} \partial_\mu \rho\, \partial_\nu \rho + \rho\, g^{\mu\nu} \partial_\mu \phi\, \partial_\nu \phi \right] - V(\rho). \tag{38}$$

Variation of the action integral with respect to the coherence phase ϕ yields the continuity equation for vacuum coherence density:

$$\nabla_\mu (\rho\, \partial^\mu \phi) = \frac{1}{\sqrt{-g}} \partial_\mu (\sqrt{-g}\, \rho\, g^{\mu\nu} \partial_\nu \phi) = 0, \tag{39}$$

ensuring conservation of vacuum coherence density.

Independent variation with respect to the density ρ yields the quantum Hamilton–Jacobi equation, identifying quantum pressure contributions:

$$\frac{\hbar^2}{2m} \frac{\Box \sqrt{\rho}}{\sqrt{\rho}} - \frac{\hbar^2}{2m} \partial_\mu \phi\, \partial^\mu \phi + \frac{dV(\rho)}{d\rho} = 0. \tag{40}$$

Defining the quantum pressure as:

$$Q(\rho) \equiv \frac{\hbar^2}{2m} \frac{\Box\sqrt{\rho}}{\sqrt{\rho}}, \tag{41}$$

the quantum Hamilton–Jacobi equation is succinctly rewritten as:

$$Q(\rho) - \frac{\hbar^2}{2m} \partial_\mu \phi \, \partial^\mu \phi + \frac{dV(\rho)}{d\rho} = 0, \tag{42}$$

clearly delineating quantum pressure, kinetic coherence-phase terms, and the vacuum potential.

Together, equations (39) and (42) fully encapsulate vacuum coherence fluid dynamics, linking fundamental quantum mechanics to cosmologically testable predictions. The continuity equation guarantees coherence-density conservation, while the quantum Hamilton–Jacobi equation encodes quantum vacuum dynamics responsible for cosmic acceleration and ripple modulations observed in the expansion history.

A.7 Ripple Structure from Global Coherence-Phase Modulation

In cosmological settings, the vacuum coherence density ρ remains nearly constant over relevant observational timescales. Starting from the continuity equation:

$$\frac{d}{dt}\left(\rho \frac{d\phi}{dt}\right) + 3H(t)\rho \frac{d\phi}{dt} = 0, \tag{43}$$

and adopting the approximation $\rho \approx$ constant, we simplify to the coherence-phase evolution equation:

$$\frac{d^2\phi}{dt^2} + 3H(t)\frac{d\phi}{dt} \approx 0, \tag{44}$$

which mirrors a classical damped harmonic oscillator. Thus, the physically meaningful solution is:

$$\phi(t) = \omega_c t + \epsilon e^{-\gamma t} \cos(\omega_m t + \phi_0), \tag{45}$$

with modulation amplitude $\epsilon \ll 1$, damping rate γ, modulation frequency ω_m, and initial phase ϕ_0. Taking the time derivative gives:

$$\frac{d\phi}{dt} = \omega_c - \epsilon e^{-\gamma t} \left[\gamma \cos(\omega_m t + \phi_0) + \omega_m \sin(\omega_m t + \phi_0) \right]. \tag{46}$$

We connect the ripple frequency ω_m to fundamental vacuum properties via the vacuum potential curvature:

$$\omega_m = \frac{\hbar}{m} \sqrt{\frac{d^2 V}{d|\Psi|^2}}, \tag{47}$$

demonstrating transparently how cosmological ripple modulation emerges from intrinsic vacuum coherence properties. The amplitude ϵ is similarly bounded by physically reasonable initial vacuum coherence conditions, analogous to known quantum-fluid cosmological scenarios [13, 45].

Transforming to redshift z using the standard cosmological relation,

$$dt = -\frac{dz}{(1+z)H(z)}, \tag{48}$$

we obtain the observationally expression for global coherence-phase modulation in the cosmic expansion rate, valid to first order in ϵ:

$$H(z) = H_0 \sqrt{\Omega_m (1+z)^3 + (1-\Omega_m)} \left[1 + \epsilon e^{-\gamma z} \sin(\omega z + \phi) \right]. \tag{49}$$

This derived form clearly demonstrates how internal coherence-phase dynamics naturally produce observational ripple modulations in the expansion rate. Unlike traditional dark-energy or modified-gravity models, this ripple signature emerges from fundamental quantum vacuum coherence dynamics, providing uniquely testable, falsifiable predictions inherent to the Genesis Field framework.

Summary of Key Derived Relations

- **Covariant Field Equation:** $\frac{\hbar^2}{2m}\Box\Psi = \frac{dV}{d\Psi^*}$
- **Continuity Equation (from $\delta\phi$ variation):** $\nabla_\mu(\rho\partial^\mu\phi) = 0$
- **Quantum Hamilton–Jacobi Equation (from $\delta\rho$):** $Q(\rho) - \frac{\hbar^2}{2m}\partial_\mu\phi\partial^\mu\phi + \frac{dV}{d\rho} = 0$
- **Quantum Pressure Definition:** $Q(\rho) = \frac{\hbar^2}{2m}\frac{\Box\sqrt{\rho}}{\sqrt{\rho}}$
- **Observable Phase Modulation in $H(z)$:** Phase coherence effects in the Genesis Field induce a ripple structure in the expansion rate, modifying the Hubble parameter as:

$$H(z) = H_0\sqrt{\Omega_m(1+z)^3 + (1-\Omega_m)}\left[1 + \epsilon\, e^{-\gamma z}\sin(\omega z + \phi)\right] \tag{50}$$

- **Ripple Structure in Energy Density:** $T_{00} \sim \rho_0\left[1 + \epsilon e^{-\gamma z}\sin(\omega z + \phi)\right]$

B KEY DEFINITIONS AND TERMINOLOGY

To ensure conceptual clarity and internal consistency, we define the principal terms used throughout the Genesis Field framework. These operational definitions form the foundation for deriving governing equations, observational predictions, and falsifiability criteria presented in this and subsequent papers.

B.1 Core Vacuum Concepts

- **Coherence:** A global quantum phase relationship maintained throughout the vacuum medium, enabling *macroscopic emergent behavior* that is distinct from stochastic quantum fluctuations. In this context, coherence refers to the long-range phase alignment of the vacuum wavefunction $\Psi(x^\mu)$ across cosmological scales.
- **Coherence Phase (ϕ):** The scalar phase of the vacuum wavefunction, encoding the

dynamical evolution of vacuum structure. Temporal variations in ϕ modulate the Hubble parameter via phase-dependent energy density terms and induce ripple-like deviations in expansion observables (see Section III).

- **Coherence Frequency (ω):** A dimensionless parameter governing the frequency of oscillations in the global coherence phase $\phi(t)$, typically defined in units of inverse logarithmic scale factor, $\omega = d\phi/d\ln a$. It can also be interpreted as the number of oscillations per Hubble time in cosmic expansion. A larger ω corresponds to finer structure in the predicted ripple.

- **Coherence Damping (γ):** A positive, dimensionless decay constant that controls the exponential damping of the ripple amplitude over cosmic time. Physically, γ represents the rate at which vacuum coherence decays due to global decoherence processes or environmental interactions. A value of $\gamma \sim 0.3$ implies significant suppression of ripple features by redshift $z \sim 0.2$.

- **Coherence Potential ($V(\rho)$):** The vacuum's self-interaction potential, governing the stability and internal dynamics of coherence. Its second derivative determines the ripple frequency through the vacuum's effective stiffness or sound speed. In this work, the specific form of V is left general, though a quartic $V(\rho) \sim \rho^2$ structure would yield $w \approx -1$ at background level.

- **Phase Modulation:** The cosmologically scaled, time-dependent evolution of the global phase $\phi(t)$, which gives rise to oscillatory features in the Hubble expansion rate $H(z)$ and luminosity distance $\mu(z)$. It originates from the vacuum's intrinsic phase dynamics as derived from the covariant Gross–Pitaevskii equation.

- **Quantum Pressure ($Q(\rho)$):** An effective repulsive term arising from spatial gradients in the vacuum density ρ, defined by $Q(\rho) = -(\hbar^2/2m)\nabla^2\sqrt{\rho}/\sqrt{\rho}$. This term acts as a stress-energy correction and contributes to late-time acceleration, analogous to the Bohm potential in quantum hydrodynamics.

B.2 Observable Predictions

- **Ripple Structure:** A model-predicted oscillatory feature in the Hubble parameter $H(z)$ and distance modulus $\mu(z)$, resulting from global coherence-phase modulation. The ripple is characterized by parameters ε (amplitude), ω (frequency), ϕ (phase offset), and γ (damping). It is a falsifiable prediction emerging from the theory's governing equations (Eq. (11)) and is tested against supernova and cosmic chronometer data in Section IV.

- **Constants as Emergent Quantities:** Fundamental constants such as the gravitational constant G, reduced Planck's constant $\hbar$, and the speed of light c are not treated as fixed parameters but are instead interpreted as emergent phenomena arising from the internal coherence of the vacuum. Variations in these constants over cosmic time are linked to the phase dynamics $\phi(t)$ and are explored in Principle V (Section II).

- **Matter as Vortex Structures:** Stable particles are hypothesized to correspond to topologically quantized vortices in the coherent vacuum wavefunction. These vortex configurations carry discrete angular momentum and persist as long-lived excitations, analogous to quantized vortices in Bose–Einstein condensates. This idea is developed in Principle III and will be formally modeled in Paper III.

C COMPUTATIONAL CODE AND VISUALIZATION

All computational analyses, numerical model fittings, ripple derivations, observational validations, and visualizations presented in this paper were developed in Python using open-source scientific libraries including `numpy`, `scipy`, `matplotlib`, `emcee`, and `corner`.

The complete, modular codebase is openly available at:

`https://github.com/genesisfield/genesisfieldmcmc`

This repository supports:

- Ripple-modulated cosmological inference using Pantheon+ and $H(z)$ datasets,
- Fixed-M calibration with SH0ES anchoring,
- Joint MCMC fitting and two-parameter ripple testing,

- Statistical comparisons including χ^2, AIC, BIC, and residual RMS,
- Full visual output generation: corner plots, residuals, ripple overlays,
- Reproducibility scripts for every figure and table in this manuscript.

This repository is currently under peer review with the *Journal of Open Source Software (JOSS)* and will be permanently archived upon acceptance. The final citation and DOI will be updated accordingly to ensure long-term reproducibility and discoverability. All numerical results, including the 4σ ripple detection and joint-fit posteriors, are reproducible using the provided configuration files and data inputs.

[1] A. G. Riess *et al.*, The Astrophysical Journal Letters **934**, L7 (2022).

[2] P. Collaboration *et al.*, Astronomy & Astrophysics **641**, A6 (2020).

[3] W. L. Freedman, The Astrophysical Journal **919**, 16 (2021).

[4] E. Di Valentino, O. Mena, S. Pan, L. Visinelli, W. Yang, A. Melchiorri, and J. Silk, Classical and Quantum Gravity **38**, 153001 (2021).

[5] R. R. Caldwell, R. Dave, and P. J. Steinhardt, Physical Review Letters **80**, 1582 (1998).

[6] J. Magueijo, Reports on Progress in Physics **66**, 2025 (2003).

[7] S. Weinberg, *Cosmology* (Oxford University Press, 2013).

[8] S. N. Bose, Zeitschrift für Physik **26**, 178 (1924).

[9] A. Einstein, Sitzungsberichte der Preussischen Akademie der Wissenschaften , 3 (1925).

[10] G. E. Volovik, *The Universe in a Helium Droplet* (Clarendon Press, 2003).

[11] E. P. Gross, Il Nuovo Cimento **20**, 454 (1961).

[12] L. P. Pitaevskii, Soviet Physics JETP **13**, 451 (1961).

[13] C. Barceló, S. Liberati, and M. Visser, Living Reviews in Relativity **8**, 12 (2005).

[14] E. Madelung, Zeitschrift für Physik **40**, 322 (1927).

[15] A. L. Fetter, Rev. Mod. Phys. **81**, 647 (2009).

[16] C. Kiefer, *Quantum Gravity* (Oxford University Press, 2009).

[17] H. D. Zeh, *The Physical Basis of the Direction of Time* (Springer-Verlag, 2007).

[18] J.-P. Uzan, Living Reviews in Relativity **14**, 2 (2011).

[19] C. J. A. P. Martins, Reports on Progress in Physics **80**, 126902 (2017).

[20] E. Schrödinger, Physical Review **28**, 1049 (1926).

[21] D. Brout, D. Scolnic, B. Popovic, A. G. Riess, J. Zuntz, *et al.*, The Astrophysical Journal **938**, 110 (2022), arXiv:2202.04077.

[22] D. M. Scolnic *et al.*, Astrophys. J. **859**, 101 (2018).

[23] M. Moresco and et al., Journal of Cosmology and Astroparticle Physics **2016** (05), 014, arXiv:1601.01701.

[24] D. Stern, R. Jimenez, L. Verde, M. Kamionkowski, and S. A. Stanford, Journal of Cosmology and Astroparticle Physics **2010** (02), 008.

[25] O. Farooq, F. Madiyar, S. Crandall, and B. Ratra, The Astrophysical Journal **835**, 26 (2017).

[26] D. Foreman-Mackey, D. W. Hogg, D. Lang, and J. Goodman, PASP **125**, 306 (2013).

[27] Planck Collaboration, N. Aghanim, Y. Akrami, M. Ashdown, J. Aumont, C. Baccigalupi, M. Ballardini, and et al., Astronomy & Astrophysics **641**, A6 (2020), arXiv:1807.06209 [astro-ph.CO].

[28] A. R. Liddle, Mon. Not. R. Astron. Soc. **377**, L74 (2007).

[29] K. P. Burnham and D. R. Anderson, *Model Selection and Multimodel Inference: A Practical Information-Theoretic Approach*, 2nd ed. (Springer, 2002).

[30] R. Laureijs, J. Amiaux, S. Arduini, J. L. Augueres, J. Brinchmann, R. Cole, M. Cropper, C. Dabin, L. Duvet, A. Ealet, *et al.*, arXiv preprint arXiv:1110.3193 (2011), arXiv:1110.3193.

[31] LSST Science Collaboration, arXiv preprint arXiv:0912.0201 (2009), arXiv:0912.0201.

[32] J. P. Gardner, J. C. Mather, M. Clampin, R. Doyon, M. A. Greenhouse, H. B. Hammel, J. B. Hutchings, P. Jakobsen, S. J. Lilly, K. S. Long, *et al.*, Space Science Reviews **123**, 485 (2006).

[33] M. Chevallier and D. Polarski, International Journal of Modern Physics D **10**, 213 (2001), arXiv:gr-qc/0009008.

[34] E. V. Linder, Physical Review Letters **90**, 091301 (2003), arXiv:astro-ph/0208512.

[35] V. Poulin, T. L. Smith, T. Karwal, and M. Kamionkowski, Physical Review Letters **122**, 221301 (2019).

[36] T. L. Smith, V. Poulin, and M. A. Amin, Physical Review D **101**, 063523 (2020).

[37] J. Solà Peracaula, A. Gómez-Valent, and C. Moreno-Pulido, Physics Reports **1044**, 1 (2023), arXiv:2203.13757 [gr-qc].

[38] F. Niedermann and M. S. Sloth, Physical Review D **103**, 043537 (2021), arXiv:2006.06686 [astro-ph.CO].

[39] K. Freese, M. W. Winkler, and G.-B. Zhao, Physical Review D **106**, 103528 (2022), arXiv:2202.09340 [astro-ph.CO].

[40] E. Di Valentino, A. Melchiorri, O. Mena, and S. Vagnozzi, Physical Review D **101**, 063502 (2020).

[41] T. Clifton, P. G. Ferreira, A. Padilla, and C. Skordis, Physics Reports **513**, 1 (2012).

[42] S. Nojiri, S. D. Odintsov, and V. Oikonomou, Physics Reports **692**, 1 (2017).

[43] D. M. Bauer, M. Lettner, C. Vo, G. Rempe, and S. Dürr, Nature Physics **11**, 276 (2015).

[44] S. Witte, K. Hornberger, and S. Nimmrichter, Physical Review Letters **118**, 123401 (2017).

[45] G. E. Volovik, *The Universe in a Helium Droplet* (Oxford University Press, Oxford, 2009).